A&A 453, 903–909 (2006)
DOI: 10.1051/0004-6361:20042382


Astronomy & Astrophysics

# Formation of compact solid water after ion irradiation at 15 K

M. E. Palumbo

INAF-Osservatorio Astrofisico di Catania, via Santa Sofia 78, 95123 Catania, Italy
e-mail: mepalumbo@oact.inaf.it

Received 17 November 2004 / Accepted 23 December 2005

**ABSTRACT**

We used infrared absorption spectroscopy to study the effects of ion irradiation on the morphology/porosity of amorphous water ice. Thin icy films (about 0.25 $\mu$m) of amorphous water were irradiated with 200 keV protons at 15 K. Both the behaviour of the OH dangling bond feature and the ability to trap carbon monoxide (CO) were used to investigate the evolution of icy samples after ion irradiation. We show that the intensity of the OH dangling bond feature decreases after ion irradiation and that the amount of absorbed carbon monoxide decreases as the fluence of impinging ions increases. The results obtained indicate that the porosity of amorphous water ice decreases after ion irradiation. Furthermore, icy mixtures such as $H_2O$:$CO_2$, $H_2O$:CO, and $H_2O$:$CH_4$ were irradiated with 200 keV $H^+$, 30 and 200 keV $He^+$ ions. Also in these cases, the intensity of the OH dangling bond band decreases after ion irradiation. However, when a second molecular species is present in the ice sample, this decrease is slower. Here we present the experimental results and discuss their relevance to our understanding of the properties of interstellar water ice. In particular, we suggest that, because of cosmic ion bombardment, water ice in interstellar grain mantles is compact in structure.

**Key words.** astrochemistry – molecular processes – methods: laboratory – ISM: lines and bands – techniques: spectroscopic – infrared: ISM

## 1. Introduction

The mid-infrared spectrum of amorphous solid water (ASW) shows absorption bands at about 3300 $cm^{-1}$ (3.03 $\mu$m; due to the O−H symmetric and anti-symmetric stretching modes), 2205 $cm^{-1}$ (4.53 $\mu$m; combination mode), 1650 $cm^{-1}$ (6.06 $\mu$m; overtone of the libration mode and H−O−H bending mode), 803 $cm^{-1}$ (12.4 $\mu$m; libration mode). In addition a small feature is present on the short wavelength wing of the O−H stretching modes band, due to OH dangling bonds (db) in the micro-pores of the amorphous structure. This feature shows two peaks at 3720 $cm^{-1}$ and 3696 $cm^{-1}$ due to two-coordinate and three-coordinate water molecules, respectively (e.g., Rowland et al. 1991).

It has been shown that amorphous water ice has a porous structure (Rowland et al. 1991) characterized by micro-pores where OH dangling groups are present. Furthermore, its morphology/porosity depends on experimental conditions such as temperature, deposition rate, and growth angle (e.g., Hagen et al. 1983; Jenniskens & Blake 1994; Kimmel et al. 2001a,b; Dohnáleck et al. 2003).

The morphology of water ice also depends on the effects of ion and UV photon irradiation. On the basis of laboratory experiments, it has been shown that polycrystalline ice is converted to amorphous ice after irradiation (Baratta et al. 1991; Moore & Hudson 1992; Leto & Baratta 2003). This effect is clearly shown by a detailed study of the 3300 $cm^{-1}$ water ice band that strongly depends on the structure of the ice sample. When amorphous ice is irradiated, a modification of the profile of the 3300 $cm^{-1}$ band is also observed (Leto et al. 1996; Leto & Baratta 2003). However, based only on the 3300 $cm^{-1}$ band no definitive conclusions can be drawn on the morphology of amorphous water after irradiation. Ion irradiation also modifies the UV-visible reflectance spectrum of water ice, and this has been attributed to rearrangement processes that affect the physical microstructure of the sample (Sack et al. 1991). Recently, molecular dynamics simulations, meant to reproduce the effects of cosmic ray bombardment of interstellar ices, have shown that a high-density phase of amorphous ice is obtained after irradiation (Guillot & Guissani 2004).

The infrared spectrum of pure carbon monoxide at low temperature shows an absorption feature at about 2140 $cm^{-1}$ (4.67 $\mu$m) due to the fundamental vibration C≡O. The profile (shape, width, and peak position) of solid CO strongly depends on the host molecules when it is mixed in with other species (e.g., Sandford et al. 1988; Palumbo & Strazzulla 1993). In particular, the band profile of CO in an $H_2O$ matrix is very peculiar, showing a main feature at about 2138 $cm^{-1}$ and a secondary feature at about 2152 $cm^{-1}$. It has been shown that both bands are due to CO molecules in the micro-pores: the 2152 $cm^{-1}$ band is due to the interaction of CO molecules with the OH dangling groups of the pore surface, while the 2138 $cm^{-1}$ feature has been tentatively identified with CO molecules interacting with the oxygen atoms of the pore-surface water molecules (e.g., Devlin 1992; Palumbo 1997; Al-Halabi et al. 2004).

Simple molecules, such as $H_2$, $N_2$, CO, Ar, and $CH_4$, absorbed in amorphous or crystalline water ice, are often used as a probe to study the properties of water ice. This can be achieved by looking at both the profile of the OH db feature present both in porous amorphous ice and on the surface of large crystalline ice clusters (Rowland et al. 1991; Hixon et al. 1992) and at the profile of the absorbed species as in the case of carbon monoxide (Devlin 1992; Palumbo 1997; Fraser et al. 2004). In addition temperature-programmed desorption studies have been used to investigate the porosity of water ice (Kimmel et al. 2001a; Dohnálek et al. 2003; Collings et al. 2003).

Here we present new experimental results meant to study the morphology of amorphous solid water after ion irradiation.

To this end we have studied, by infrared transmission spectroscopy, the diffusion of CO in irradiated amorphous water and the effects of ion irradiation on ice mixtures. This article is organised as follows: Sect. 2 describes the experimental set-up; the results are presented in Sect. 3, and the astrophysical applications are discussed in Sect. 4.

## 2. Experimental set-up

Icy samples were prepared in a stainless steel vacuum chamber, schematically depicted in Fig. 1, where pressure was kept at $10^{-7}$ mbar. A crystalline silicon substrate, was placed in thermal contact with a cold finger whose temperature can be varied between 300 K and 10 K.

The vacuum chamber could be placed in the sample compartment of an infrared spectrometer (Bruker Equinox 55), and transmission spectra were obtained through the KBr windows and a hole in the final tail of the cold finger, which allowed the infrared beam to transmit through the substrate and the sample. A leak valve was used to admit gaseous species into the chamber, where they froze out on the substrate. The gas inlet was not directed towards the substrate, thus a "background deposition" was obtained. A He-Ne laser ($\lambda$ = 540 nm) was used to monitor the thickness of the ice film during accretion. This was achieved by looking at the interference pattern (intensity versus time) given by the laser beam reflected at an angle of 45° both by the vacuum-film and film-substrate interfaces (Baratta & Palumbo 1998).

The vacuum chamber was interfaced to an ion implanter (200 kV; Danfysik) from which ions with energy up to 200 keV (400 keV for double ionisations) could be obtained. Results presented in this paper were obtained using 200 keV $H^+$, 30 and 200 keV $He^+$ ions. In all experiments the penetration depth of impinging ions was larger than the ice sample thickness. The ion beam produced a larger spot on the target than the area probed by the infrared beam. A current integrator on the path of the ion beam measured the charge that reached the sample during irradiation. Ion current density ranged between 100 nA cm$^{-2}$ and few $\mu$A cm$^{-2}$ in order to avoid a macroscopic heating of the sample. The substrate holder formed an angle of 45° degrees both with the infrared beam and the ion beam. This configuration offered the advantage that spectra can be taken in situ, even during irradiation, without tilting the sample.

A rotatable polarizer was placed in the path of the infrared beam. This gave the opportunity of recording spectra with the electric vector parallel (P polarized) and perpendicular (S polarized) to the plane of incidence. The plane of incidence is the plane of the paper in Fig. 1; this plane contains P polarized light, while the plane of S polarization is perpendicular to the paper. As shown by Baratta et al. (2000) spectra recorded at oblique incidence in S polarization are equivalent to spectra at normal incidence. All spectra here shown were ratioed to a background spectrum that includes the substrate and were taken with a resolution of 1 cm$^{-1}$.

## 3. Results

### 3.1. Ion irradiation of ASW

Amorphous solid water (ASW) samples were obtained at 15 K. The thickness of the icy films was about 0.25 $\mu$m. Figure 2 shows the infrared transmission spectrum (in optical depth scale) of amorphous water ice in the 3800–3600 cm$^{-1}$ spectral region. Two bands at 3697 cm$^{-1}$ and 3720 cm$^{-1}$ are present that are due to the O−H dangling bonds (db) in porous amorphous ice. These bands are attributed to three- and two-coordinate water molecules, respectively (Rowland et al. 1991). The OH db feature is superposed on the wing of the strong broad band due to O−H stretching modes at about 3300 cm$^{-1}$.

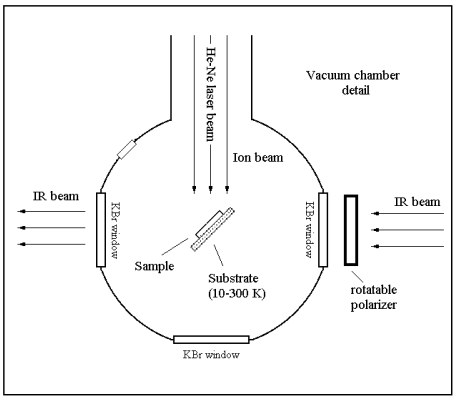


**Fig. 1.** Schematic depiction (*top view*) of the vacuum chamber.

**Table 1.** Peak position of the OH dangling bond features. In a few instances the two- and three-coordinate peaks merge into one broad feature.

| sample | OH db peak positions (cm$^{-1}$) | Ref. |
|---|---|---|
| pure $H_2O$ | 3695, 3720 | 1, 2 |
| $H_2O$:$N_2$ | 3672, 3694 | 1, 3 |
| $H_2O$:$O_2$ | 3669, 3694 | 2 |
| $H_2O$:$H_2O_2$ | 3664 | 2 |
| $H_2O$:$CO_2$ | 3657 | 2 |
| $H_2O$:CO | 3636 | 2 |
| $H_2O$:$CH_4$ | 3669, 3684 | 2 |
| $H_2O$:$SO_2$ | 3676 | 2 |

1. Rowland et al. (1991); 2. this work; 3. Palumbo & Strazzulla (2003).

As already discussed in the literature, the profile of the OH db feature changes if another species is mixed in with water ice. In fact several laboratory experiments have been perfomed that show that the OH db feature shifts when other species are absorbed in water ice (e.g., Rowland et al. 1991; Devlin et al. 1992; Palumbo & Strazzulla 2003; Palumbo 2005). Table 1 reports the position of the OH db feature in different $H_2O$:X mixtures. In a few instances the two- and three-coordinate peaks merge in one broad feature. In the case of the mixture $H_2O$:$CO_2$, three different mixtures were studied, namely 1:1, 5:1 and 10:1. Laboratory spectra show that the profile of the OH db band does not depend on the $H_2O/CO_2$ ratio. Similarly, in the case of the mixture $H_2O$:CO two different mixtures were studied, namely 2:1 and 10:1. Again the profile of the OH db band does not depend on the $H_2O$/CO ratio.

Spectra of amorphous water were taken after irradiation with 200 keV $H^+$ ions at different fluences. Figure 2 shows that the intensity of the OH db feature decreases after ion irradiation. This is attributed to the loss of OH dangling groups in the micropores, which in turns means a modification of the structure of the icy sample. This effect was reported by Raut et al. (2004) who grew a water ice film at 80 K and irradiated it with 100 keV protons. These authors interpret the ion induced pore collapse as the effect of annealing in the transiently "hot" region around the ionization track produced by each individual ion.

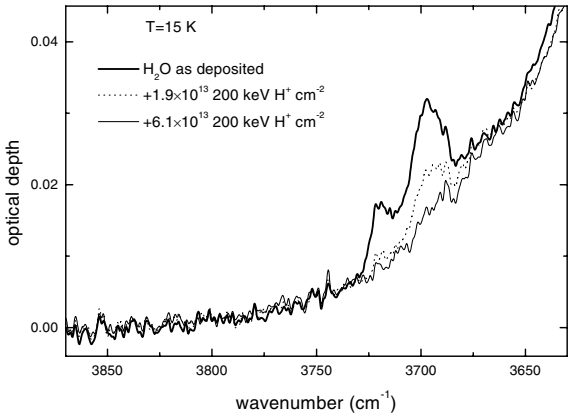


**Fig. 2.** Profile of the OH db band in pure amorphous $H_2O$ ice before and after irradiation with 200 keV protons at 15 K.

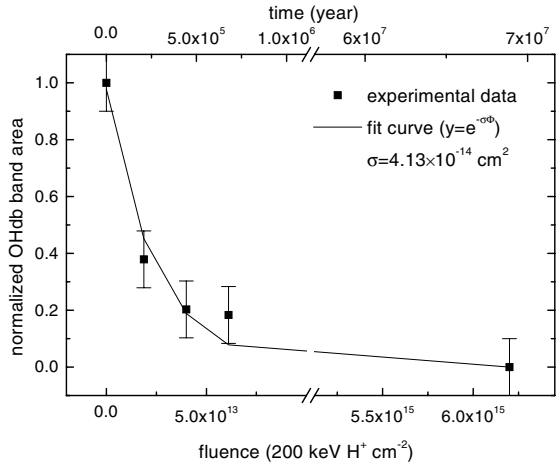


**Fig. 3.** Normalized integrated intensity of the OH db feature of pure $H_2O$ after ion irradiation with 200 keV $H^+$ ions. Experimental data have been fitted with an exponential curve $y = e^{-\sigma\Phi}$ where $\Phi$ is the ion fluence in ions $cm^{-2}$ and $\sigma$ is the cross section in $cm^2$.

Figure 3 shows the integrated intensity (area) of the OH dangling bond feature normalized to the initial value as a function of ion fluence. Experimental data were fitted with an exponential curve $y = e^{-\sigma\Phi}$ where $\Phi$ is the ion fluence in ions $cm^{-2}$. From the fit the resulting cross section is $\sigma = 4.13 \times 10^{-14}$ $cm^2$. The top x-axis indicates the time (years) that would be necessary to obtain the same effects in dense interstellar clouds (see Sect. 4).

### *3.2. CO diffusion in irradiated ASW*

In order to verify if ion irradiation causes a reduction of the porosity of the amorphous water ice sample, we measured the capability of irradiated amorphous water ice to absorb CO molecules.

It has already been shown that if CO is deposited on top of an amorphous water ice film, and as the sample is warmed up, CO molecules diffuse in the ice underneath (e.g., Devlin 1992; Palumbo 1997; Collings et al. 2003). The diffusion of CO in ASW is clearly shown by a modification of the CO-band profile. Figure 4 (top panel) shows the transmission spectra taken in S polarization (plotted in optical depth scale) of a CO thin film deposited on top of an amorphous water ice sample at 15 K and after being warmed up to 30 K. Figure 4 (bottom panel) shows the spectra in P polarization of the same sample. In

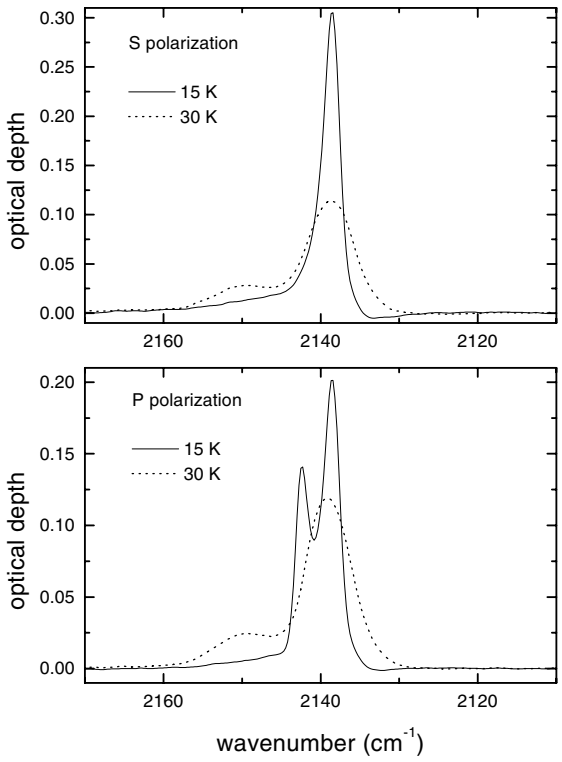


**Fig. 4.** Profile of the 2140 $cm^{-1}$ CO band in P and S polarizations after deposition on top of a water ice layer at 15 K (solid lines) and after diffusion in the water ice sample (dotted lines).

S polarization at 15 K, the CO band peaks at 2138 $cm^{-1}$ with FWHM (Full Width at Half Maximum) equal to 3 $cm^{-1}$. After warm-up the profile changes: a new peak appears at 2152 $cm^{-1}$ and FWHM values 7 $cm^{-1}$. These changes are considered as the proof of diffusion in the water ice underneath (Devlin 1992; Palumbo 1997; Collings et al. 2003; Fraser et al. 2004).

In P polarization the profile of the CO film deposited on amorphous water ice shows an additional feature at 2142 $cm^{-1}$ (bottom panel in Fig. 4). It has been shown (Baratta & Palumbo 1998) that this latter feature does not correspond to any peak in the imaginary part ($k$) of the complex refractive index and is related to the strong variation of the real part $n$ that is less than 1 in the region across the absorption band. This effect is present in the case of strong absorption bands. These observed features are also known as the transversal optical (TO; at 2138 $cm^{-1}$) and longitudinal optical (LO; at 2142 $cm^{-1}$) modes. As discussed by Palumbo et al. (2006), the relative intensity of these two features depends on the optical properties of the surface on which CO is deposited.

After diffusion the CO band profile in P and S polarization becomes very similar. In fact when CO molecules are diluted in water ice, the $k$ values across the CO band decreaes. It has already been shown that in the case of weak bands P and S spectra are indistinguishable (Baratta et al. 2000).

In the conditions of our experimental set-up, diffusion takes place at about 26 K and pure CO ice deposited on the bare substrate sublimes at about 30 K. If diffusion takes place and a $H_2O$:CO mixture is obtained, CO remains partially trapped in $H_2O$ at higher temperatures and up to the crystallization temperature of water ice (about 150 K; Schmitt et al. 1989; Kimmel et al. 2001a; Fraser et al. 2004; Collings et al. 2004).

A further independent proof of diffusion of CO in ASW is given by the profile of the OH db feature. In fact after diffusion

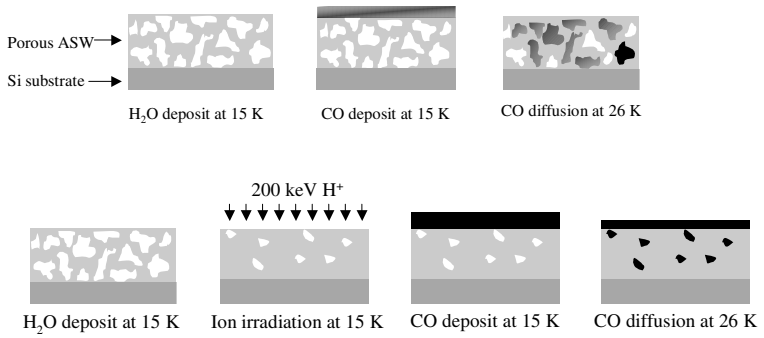


**Fig. 5.** Schematic depiction of the experimental procedure followed to study the fraction of CO diffused in irradiated amorphous solid water.

this feature shifts to 3636 $cm^{-1}$. This is the same position of the OH db feature as in a $H_2O$:CO co-deposited mixture (Table 1). It is important to note that, if CO is deposited on the bare Si substrate, none of the band profile modification described above is observed after warm up. In particular the 2152 $cm^{-1}$ feature does not appear and no CO is left over on the substrate at 30 K.

As schematically shown in Fig. 5, CO was deposited in the first experiment on top of the water ice sample at 15 K and then the sample was warmed up to 26 K. At this temperature CO molecules diffuse in the porous ice underneath and an $H_2O$:CO mixture is obtained. Then the temperature of the sample was raised in a stepwise fashion up to the water sublimation temperature. Transmission infrared spectra, in P and S polarizations, were recorded at each step of this procedure. In the irradiation experiments, the water ice sample was irradiated with 200 keV $H^+$ ions. After irradiation, CO was deposited on top of the irradiated ice at 15 K and then the sample warmed up to allow diffusion of CO in the ice underneath. Again, transmission infrared spectra, in P and S polarization, were recorded at each step of this procedure. This experimental procedure was repeated in order to test the diffusion of CO in water ice samples irradiated at different ion fluences.

Figure 6 reports the fraction of deposited CO that diffuses in water ice underneath after the ice sample was irradiated with 200 keV protons. It is evident that this fraction decreases as the ion fluence increases. At the highest fluence investigated ($6.2 \times 10^{15}$ 200 keV $H^+$ $cm^{-2}$), no CO molecules are absorbed in the water sample, within the errorbars. Thus we conclude that the porosity of amorphous water ice decreases after ion irradiation. The solid line in Fig. 6 is a fit of the experimental data with an exponential curve $y = e^{-\sigma\Phi}$ where $\Phi$ is the ion fluence in ions $cm^{-2}$. From the fit the resulting cross section is $\sigma = 1.14 \times 10^{-14}$ $cm^2$. It is interesting to note that this value is about four times lower than the cross section obtained from the fit of the data relative to the decrease of the OH db feature (see Fig. 3). Further experiments will be necessary to understand if this difference is real or if these values are the same within the errorbars. The top $x$-axis of Fig. 6 indicates the time (years) that would be necessary to obtain the same effects in interstellar dense molecular clouds (see Sect. 4).

In all the experiments described above the same amount of CO was deposited on top of each of the irradiated water ice samples at 15 K. This amount was estimated in each experiment from the integrated intensity of the CO band in the spectrum taken at 15 K. After warming up to 26 K, the fraction of CO that does not diffuse in the water ice underneath remains on top of the ice sample. In order to estimate the fraction of diffused CO, the samples were further warmed up to 30 K in order to cause the sublimation of non-diffused CO. It was verified in a few blank

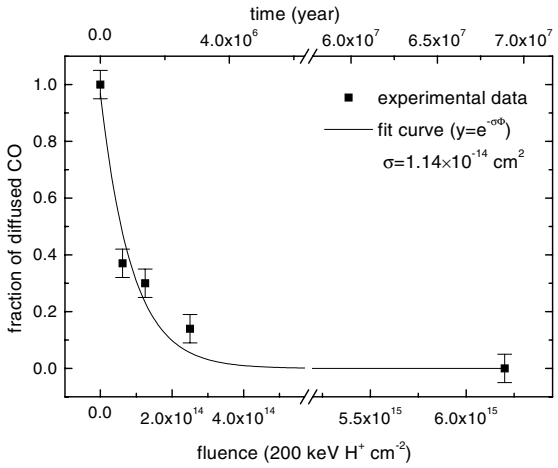


**Fig. 6.** Fraction of deposited CO that diffuses at 26 K in water ice after the ice sample has been irradiated at 15 K with 200 keV $H^+$, as a function of ion fluence. Experimental data have been fitted with an exponential curve $y = e^{-\sigma\Phi}$ where $\Phi$ is the ion fluence in ions $cm^{-2}$ and $\sigma$ is the cross section in $cm^2$.

experiments that the band profile due to diffused CO does not change if the temperature varies from 26 to 30 K. Following Gerakines et al. (1995), the same integrated absorbance for the CO band (i.e., $1.1 \times 10^{-17}$ cm $mol^{-1}$) was used in all experiments and at all temperatures.

### 3.3. Blank experiments

It is well known that ion irradiation of pure solid $H_2O$ causes the formation of $H_2O_2$, $H_2$, OH, and $O_2$ (e.g., Johnson 1990; Moore & Hudson 2000; Baragiola et al. 2003; Gomis et al. 2004), thus some blank experiments are necessary to verify that the results discussed above are due to a change in the morphology of water ice and do not depend on the presence of other species in the porous structure of solid water. As discussed above (see Table 1), the OH db feature shifts when other species are mixed in with water ice (e.g., Rowland et al. 1991; Devlin et al. 1992; Palumbo & Strazzulla 2003; Palumbo 2005). Other cases have been reported in the literature of species (such as $H_2$, $CH_4$, Ar, $N_2$, CO, $CF_4$, and ethylene oxide) absorbed in $D_2O$ (Rowland et al. 1991; Devlin 1992). It is interesting to note that in none of the mixtures investigated does the OH (OD) dangling bond feature disappear, so that the decrease in the intensity of the OH db feature after ion irradiation cannot be ascribed to the formation of other molecular species in the water ice sample.

We also verified whether the presence of other species in the porous structure of amorphous water prevent the diffusion

of CO after ion irradiation. In particular we considered a co-deposited mixture $H_2O$:$O_2$ (with about 20% of $O_2$) and verified that CO diffuses in this mixture following the same procedure as described above. However, given that molecular oxygen has no intense infrared bands so we cannot verify that $O_2$ sublimates at the temperature at which CO diffuses in the water matrix we also considered an $H_2O$:$CO_2$ = 8:1 mixture. In fact $CO_2$ has intense infrared bands and its sublimation temperature is higher than the CO diffusion temperature. Following the same procedure described above for the diffusion of CO in solid amorphous water, we found that 100% of CO diffuses in a co-deposited $H_2O$:$CO_2$ mixture. Thus we conclude that the presence of other molecules in the porous structure of amorphous water does not prevent the diffusion of CO.

It has been discussed in Loeffler et al. (2005) that $H_2O$ and $CO_2$ can condense on the cold sample during irradiation experiments. In order to verify whether a layer of $CO_2$ on top of solid $H_2O$ could prevent the diffusion of CO after ion irradiation, we performed the following experiment. First, we deposited a water ice sample (about 100 nm thick) at 15 K. Second, we deposited a $CO_2$ layer (about 6 nm thick) on top of the water ice sample at 15 K. Third, we deposited a CO layer (about 40 nm) on top of the $CO_2$-on-$H_2O$ sample. Then, we warmed up the sample to 26 K and verified that 100% of CO diffuses in water ice. This means that the $CO_2$ layer on top of the water ice sample does not prevent diffusion of CO.

On the basis of all the experimental results, we conclude that CO molecules do not diffuse in amorphous solid water after ion irradiation because the morphology of the amorphous water ice is modified by irradiation itself.

### 3.4. Irradiation of mixtures

Spectra of a few co-deposited $H_2O$:X mixtures at 15 K before and after ion irradiation were also taken. In particular $H_2O$:CO, $H_2O$:$CO_2$, and $H_2O$:$CH_4$ mixtures were studied. These co-deposited mixtures were irradiated with 200 keV $H^+$, 30 and 200 keV $He^+$ ions at 15 K.

Figure 7 shows the integrated intensity (band area) of the OH db feature after ion irradiation divided by the initial value. In order to compare results for different mixtures irradiated with different ions the normalized band area was plotted versus dose, that is the energy released per 16 amu (atomic mass units), as suggested by Strazzulla & Johnson (1991). Doses were estimated using the stopping power values (S in eV cm$^2$ molecule$^{-1}$) reported in Table 2 (Ziegler 2003). In the same figure the integrated intensity of the OH db feature after ion irradiation of pure water ice is also reported for comparison. It is evident that the intensity of the OH db feature also decreases after ion irradiation in the case of co-deposited mixtures. However, this decrease is slower with respect to the case of pure amorphous water ice. The top $x$-axis of Fig. 7 indicates the time (years) that would be necessary to obtain the same effects in dense interstellar clouds (see Sect. 4).

The fact that the OH db sites are not completely lost after ion irradiation of mixtures is also evident from the profile of the CO feature in the case of the co-deposited $H_2O$:CO mixtures. As already reported by Palumbo & Strazzulla (1993) and Palumbo (1997), the intensity of the 2152 cm$^{-1}$ band decreases with respect to the main 2139 cm$^{-1}$ band after ion irradiation but does not disappear after the highest doses investigated following the same behaviour of the OH db feature.

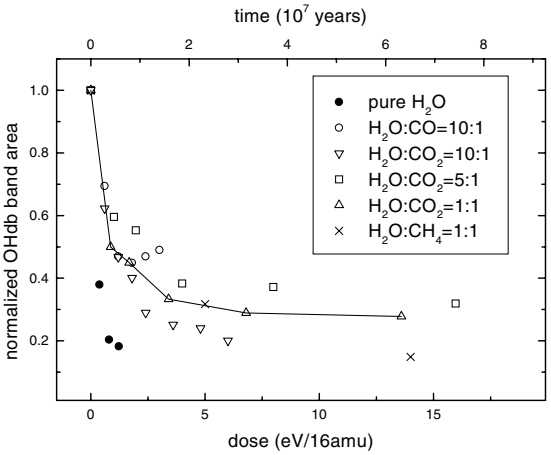


**Fig. 7.** Behaviour of the OH db feature in different ice mixtures after ion irradiation with 200 keV $H^+$, 30 and 200 keV $He^+$ ions. In order to compare results obtained after irradiation of different mixtures with different ions, the ion fluences (ions cm$^{-2}$) have been converted to dose (eV/16 amu) using the stopping power values reported in Table 2. A solid line that connects the points relative to the $H_2O$:$CO_2$ = 1:1 mixture has been drawn to guide the eyes.

**Table 2.** Stopping power values (S) adopted in this work.

| Mixture | Ion and energy | $S$ $10^{-15}$eV cm$^2$ molecule$^{-1}$ |
|---|---|---|
| $H_2O$ | $H^+$, 200 keV | 22.5 |
| $H_2O$ | $H^+$, 1 MeV | 7.8 |
| $H_2O$:CO = 10:1 | $H^+$, 200 keV | 250.3 |
| $H_2O$:CO = 10:1 | $H^+$, 1 MeV | 88.2 |
| $H_2O$:$CO_2$ = 1:1 | $He^+$, 200 keV | 175.5 |
| $H_2O$:$CO_2$ = 5:1 | $He^+$, 200 keV | 445.8 |
| $H_2O$:$CO_2$ = 10:1 | $H^+$, 200 keV | 265.1 |
| $H_2O$:$CO_2$ = 10:1 | $H^+$, 1 MeV | 93.9 |
| $H_2O$:$CH_4$ = 1:1 | $He^+$, 30 keV | 67.8 |

## 4. Discussion

It is generally accepted that interstellar water ice forms because of surface reactions on grain mantles at low temperature (about 10 K). Thus interstellar water ice is believed to be mainly amorphous (Hagen et al. 1981). However, we know very little about its morphology and, in particular, its porosity. It has been suggested (e.g., McCoustra & Williams 1996) that the detection of the OH dangling bond feature in interstellar spectra would have given important information on the properties of water ice. This feature was predicted to have a detectable strength and should have been seen with the Infrared Space Observatory (ISO). However, so far, no clear detection of this feature has been reported (e.g., Keane et al. 2001).

A detailed study (Fraser et al. 2004) of the profile of the interstellar solid CO band based on high signal-to-noise ratio observations towards low-mass stars forming clouds (Pontoppidan et al. 2003) indicates that interstellar water ice is compact. Laboratory experiments have shown that when carbon monoxide is mixed in with water ice a feature appears at 2152 cm$^{-1}$ due to the interaction of CO with OH dangling bonds (e.g., Sandford et al. 1988; Devlin 1992; Palumbo 1997). This feature has been extensively searched for in the spectra of interstellar ices and never detected. The good quality of available observations leads to the conclusion that interstellar solid CO molecules do no interact with the OH dangling bonds of solid water (Pontoppidan et al. 2003; Fraser et al. 2004). The compact nature of interstellar

water ice and then the absence of any OH dangling bond could be one possible explanation for the non detection of the 2152 $cm^{-1}$ feature. Furthermore the asymmetric profile of the interstellar CO feature presents a component at 2136 $cm^{-1}$. This was formerly known as the broad component or polar component (e.g. Tielens et al. 1991; Chiar et al. 1995; Teixeira et al. 1998). After Pontoppidan et al. (2003) this is known as the red component. Based on laboratory spectra this component has been attributed by Fraser et al. (2004) to solid CO embedded in compact water ice. The existence of compact ice would prevent small molecules (such as CO) to diffuse into water ice. This is consistent with the hyphothesis that the 2139 $cm^{-1}$ component of the observed interstellar solid CO feature is due to CO-ice layers accreted on other ice layers. This suggests that CO-$H_2O$ containing interstellar ices are best represented by a layered ice model rather than a mixed ice (Fraser et al. 2004).

It is possible that after surface reactions only compact amorphous water ice forms on interstellar grains. Alternatively, we have presented experimental results showing that after ion irradiation the porous structure of water ice collapses so the ice becomes compact.

In order to estimate the time necessary to obtain the effects observed in laboratory in interstellar dense clouds we consider the approximation of monoenergetic 1 MeV protons and assume that in dense interstellar regions the 1 MeV proton flux is equal to 1 proton $cm^{-2}$ $s^{-1}$ (see Mennella et al. 2003 for a detailed discussion). However our experimental results were obtained using 200 keV protons. Thus in order to extrapolate the laboratory results to the interstellar medium conditions we assumed that they scale with the stopping power ($S$) of impinging ions. As reported in Table 2, $S(200\ \mathrm{keV})/S(1\ \mathrm{MeV})$ is 2.9 in the case of pure water ice. With these hypotheses in mind we have indicated in Figs. 3, 6, and 7 timescale axes (top $x$-axis), which give an estimation of the time (years) necessary to obtain the effects, observed in laboratory, on interstellar ices. As reported by Greenberg (1982) a dense-cloud lifetime ranges between $3 \times 10^7$ and $5 \times 10^8$ years. Assuming $n_0 \sim 10^4$ $cm^{-3}$, the gas takes $10^9/n_0 \simeq 10^5$ years to condense on grains (Tielens & Allamandola 1987). Thus, icy grain mantles suffer cosmic ion irradiation for about $10^5$–$10^8$ years. The first estimate refers to the case of icy mantles that sublime as soon as they are formed (which could be the case for volatile species such as CO), while the second estimate refers to the limit case of icy mantles that survive the whole cloud lifetime (which could be the case for less volatile species such as $H_2O$). Figure 3 shows that after about $1 \times 10^6$ years the integrated intensity of the OH dangling bond feature is reduced to 10% of the value it would have without the effects of cosmic ion bombardment. This period is shorter than the estimated lifetime of water ice mantles in dense clouds. Thus on the basis of laboratory results, we suggest that because of cosmic ion irradiation, interstellar water ice is amorphous and non porous. Then the OH db feature is not observed in interstellar ices because its intensity is reduced by cosmic ion irradiation.

We have shown that after ion irradiation the porous structure of water ice collapses and the ice becomes compact. This prevents small molecules (such as CO) diffusing into water ice. However, this compacting process is slower and could never be completed during the cloud lifetime, if another species is mixed in with water ice. Let us now discuss which observational evidence we do have that other species are not mixed in with water ice in interstellar icy grain mantles.

An earlier study of the profile of the 9.7 and 8.9 $\mu$m features of solid $CH_3OH$, towards the deeply embedded protostar GL2136, indicates that the observed profile is consistent with a high $CH_3OH/H_2O$ abundance ratio (>0.5), while from the columm density a low (~0.1) abundance ratio was derived. This led to the conclusion that solid methanol and water ice are located in independent grain components in dense clouds (Skinner et al. 1992). Recently, a similar conclusion has been drawn after a comparison of laboratory spectra with the 3.54, 3.84, 3.94 $\mu$m bands, observed towards high-mass protostars, and attributed to the $CH_3$ symmetric stretching and combination modes of solid methanol (Dartois et al. 1999). Also a detailed study of the profile of the carbonyl sulphide (OCS) feature at 4.9 $\mu$m showed that a good match is obtained between the observed profile and that of a laboratory spectrum of a $CH_3OH$:OCS ice mixture rather than a water-rich ice mixture (Palumbo et al. 1995, 1997).

The observed band profiles due to solid CO and $CO_2$ indicate the presence of different components along the line of sight. As discussed above comparisons of laboratory spectra with the observed solid CO band suggest the presence of CO embedded in compact solid water (Pontoppidan et al. 2003; Fraser et al. 2004). As concerns solid $CO_2$, observations towards high mass star-forming regions indicate that some of the observed carbon dioxide is segregated (e.g., Ehrenfreund et al. 1998; Gerakines et al. 1999). On the other hand, recent observations towards field stars indicate that most of solid $CO_2$ is intimately mixed with water ice (e.g., Whitthet et al. 1998; Bergin et al. 2005). As shown by Mennella et al. (2004, 2006), CO and $CO_2$ form easily after ion irradiation and UV photolysis of carbon grains covered by water ice. Furthermore, Mennella et al. have shown that the CO and $CO_2$ laboratory band profiles are good spectroscopic analogs of the observed polar components of both the CO and $CO_2$ band profiles. This result would explain the presence of CO and $CO_2$ embedded in compact water ice and simultaneously the smooth profile of the 3 $\mu$m interstellar water ice band. Furthermore this would explain why the 2152 $cm^{-1}$ band and the OH dangling bond feature have not been detected in interstellar spectra.

*Acknowledgements.* I would like to thank F. Spinella for his technical assistance during laboratory measurements and G.A. Baratta for helpful discussions during the preparation of this work. This research was supported by the Italian Ministero dell'Istruzione, dell'Università e della Ricerca (MIUR).

## References

Al-Halabi, A., Fraser, H. J., Kroes, G. J., & van Dishoeck, E. F. 2004, A&A, 422, 777
Baragiola, R. A., Vidal, R. A., Svendsen, W., et al. 2003, NIMB, 209, 294
Baratta, G. A., & Palumbo, M. E. 1998, J. Opt. Soc. Am A, 15, 3076
Baratta, G. A., Leto, G., Spinella, F., Strazzulla, G., & Foti, G. 1991, A&A, 252, 421
Baratta, G. A., Palumbo, M. E., & Strazzulla, G. 2000, A&A, 357, 1045
Bergin, E. A., Melnick, G. J., Gerakines, P. A., Neufeld, D. A., & Whittet, D. C. B. 2005, ApJ, 627, L33
Chiar, J. E., Adamson A. J., Kerr, T. H., & Whittet, D. C. B. 1995, ApJ, 455, 234
Collings, M. P., Dever, J. W., Fraser, H. J., McCoustra, M. R. S., & Williams, D. A. 2003, ApJ, 583, 1058
Collings, M. P., Anderson, M. A., Chen, R., et al. 2004, MNRAS, 354, 1133
Dartois, E., Schutte, W., Geballe, T. R., et al. 1999, A&A, 342, L32
Devlin, J. P. 1992, J. Phys. Chem., 96, 6185
Dohnálek, Z., Kimmel, G. A., Ayotte, P., Smith, R. S., & Kay, B. D. 2003, J. Chem. Phys., 118, 364
Ehrenfreund, P., Dartois, E., Demyk, K., & d'Hendecourt, L. 1998, A&A, 339, L17
Fraser, H. J., Collings, M. P., Dever, J. W., & McCoustra, M. R. S. 2004, MNRAS, 353, 59
Gerakines, P. A., Schutte, W. A., Greenberg, J. M., & van Dishoeck, E. F. 1995, A&A, 296, 810
Gerakines, P. A., Whittet, D. C. B., Ehrenfreund, P., et al. 1999, ApJ, 522, 357
Gomis, O., Leto, G., & Strazzulla, G. 2004, A&A, 420, 405
Greenberg, M. 1982, in Comets, ed. L. L. Wilkening (Tucson: The University of Arizona Press), 131

Guillot, B., & Guissani, Y. 2004, J. Chem. Phys., 120, 4366
Hagen, W., Tielens, A. G. G. M., & Greenberg, J. M. 1981, Chem. Phys., 56, 267
Hagen, W., Tielens, A. G. G. M., & Greenberg, J. M. 1983, A&AS, 51, 389
Hixson, H. G., Wojcik, M. J., Devlin, M. S., Devlin J. P., & Buch, V. 1992, J. Chem. Phys. 97, 753
Jenniskens, P., & Blake, D. 1994, Science, 265, 753
Johnson, R. E. 1990, Energetic charged particle interactions with atmospheres and surfaces (Springer Verlag Press)
Keane, J. K., Boogert, A. C. A., Tielens, A. G. G. M., Ehrenfreund, P., & Schutte, W. A. 2001, A&A, 375, L43
Kimmel, G. A., Stevenson, K. P., Dohnálek, Z., Smith, R. S., & Kay, B. D. 2001a, J. Chem. Phys., 114, 5284
Kimmel, G. A., Dohnálek, Z., Stevenson, K. P., Smith, R. S., & Kay, B. D. 2001b, J. Chem. Phys., 114, 5295
Leto, G., & Baratta, G. A. 2003, A&A, 397, 7
Leto, G., Palumbo, M. E., & Strazzulla, G. 1996, Nucl. Instr. Meth. B, 116, 49
Loeffler, M. J., Baratta, G. A., Palumbo, M. E., Strazzulla, G., & Baragiola, R. A. 2005, A&A, 435, 587
McCoustra, M., & Williams, D. A. 1996, MNRAS, 279, L53
Mennella, V., Baratta, G. A., Esposito, A., Ferini, G., & Pendleton, Y. J. 2003, ApJ, 587, 727
Mennella, V., Palumbo, M. E., & Baratta, G. A. 2004, ApJ, 615, 1073
Mennella, V., Baratta, G. A., Palumbo, M. E., & Bergin, E. A. 2006, ApJ, 643, 923
Moore, M. H., & Hudson, R. L. 1992, ApJ, 401, 353
Moore, M. H., & Hudson, R. L. 2000, Icarus, 145, 282
Palumbo, M. E. 1997, J. Phys. Chem. A, 101, 4298
Palumbo, M. E. 2005, J. Phys. Conf. Ser., 6, 211
Palumbo, M. E., & Strazzulla, G. 1993, A&A, 269, 568
Palumbo, M. E., & Strazzulla, G. 2003, Can. J. Phys., 81, 217
Palumbo, M. E., Tielens, A. G. G. M., & Tokunaga, A. T. 1995, ApJ, 449, 674
Palumbo, M. E., Geballe, T. R., & Tielens, A. G. G. M. 1997, ApJ, 479, 839
Palumbo, M. E., Baratta, G. A., Collings, M., & McCoustra, M. 2006, Phys. Chem. Chem. Phys., 8, 279
Pontoppidan, K. M., Fraser, H. J., Dartois, E., et al. 2003, A&A, 408, 981
Raut, U., Loeffler, M. J., Vidal, R. A., & Baragiola, R. A. 2004, LPI, 35, 1922
Rowland, B., Fisher, M., & Devlin, J. P. 1991, J. Chem. Phys., 95, 1378
Sack, N. J., Boring, J. W., Johnson, R. E., Baragiola, R. A., & Shi, M. 1991, J. Geophys. Res., 96, 17, 535
Sandford, S. A., Allamandola, L. J., Tielens, A. G. G. M., & Valero, G. J. 1988, ApJ, 329, 498
Schmitt, B., Greenberg, M. J., & Grim, R. J. A. 1989, ApJ, 340, L33
Skinner, C. J., Tielens, A. G. G. M., Barlow, M. J., & Justtanont, K. 1992, ApJ, 399, L79
Strazzulla, G., & Johnson, R. 1991, in Comets in the post Halley era, ed. R. L. Newburn, & M. Neugebauer (Kluwer, Dordrecht), 243
Teixeira, T. C., Emerson, J. P., & Palumbo, M. E. 1998, A&A, 330, 711
Tielens, A. G. G. M., & Allamandola, L. J. 1987, in Physical processes in interstellar clouds, ed. G. E. Morfill, & M. Scholer (Reidel, Dordrecht), 333
Tielens, A. G. G. M., Tokunaga, A. T., Geballe, T. R., & Baas, F. 1991, ApJ, 381, 181
Whittet, D. C. B., Gerakines, P. A., Tielens, A. G. G. M., et al. 1998, ApJ, 498, L159
Ziegler, J. F. 2003, Stopping and Range of Ions in Matter SRIM2003 (available at `www.srim.org`)